2007 IEEE International Conference on
Robotics and Automation
Roma, Italy, 10-14 April 2007

The Effect of Semicircular Feet on Energy Dissipation by Heel-strike in Dynamic Biped Locomotion

Fumihiko Asano and Zhi-Wei Luo

Abstract— **This paper investigates the effect of semicircular feet on dynamic bipedal walking. It has been clarified in [3] that underactuated virtual passive dynamic walking can be realized by using the rolling effect, which acts as the ankle-joint torque virtually. It has been also shown that, throughout parameter studies, the rolling effect dramatically increases the stable domain of limit cycles. Now that the effect of semicircular feet during stance phase has been discussed, this paper then focuses the effect on mechanical energy dissipation by heel-strike. It is theoretically clarified that, through modeling and analysis of an inelastic collision, increasing walking speed is achieved not by the rolling effect during stance phase but by the effect of reducing mechanical energy dissipation by heel-strike.**

I. Introduction

Energy-efficient and high-speed dynamic biped locomotion is a recent major subject in the research area of robotic biped locomotion. Passive dynamic walking (PDW) [2] is an influential candidate and many PDW-inspired control approaches and walking machines have been proposed so far. Semi-active dynamic walkers with small or un-powerful actuators seem to be a natural solution as an extension of PDW to level walking. One of the characteristic that, however, most distinguishes passive-dynamic walkers from recent biped humanoid robots is the feet whose shape is circular or convex curve. The robots with such foot shape in contact with the ground at exactly one point which is equivalent to the zero moment point (ZMP) [1], and such contact style is a feature of *ZMP-free robots* in the meaning of motion control without using ankle-joint torque actively.

The authors have clarified that the rolling effect of semicircular feet can be transformed to the ankle-joint torque of a flat feet model in the case of linearized system, and this enables the robot to walk on level ground by only hip-joint actuation which reproduces virtual gravity effect [3]. The ankle-joint torque is in general most effective to accelerate the robot's center of mass (CoM) forward and semicircular feet can reproduce this effect, whereby the robot can act as a fully-actuated system virtually. This paper first introduces two planar biped models and underactuated virtual passive dynamic walking to show the basic rolling effect during the stance phase.

The authors have discovered that semicircular feet are also effective in inelastic collisions of heel-strike for improvement of the walking system performance in the meaning of decreasing the mechanical energy dissipation. In the previous works on PDW, however, only the effect during stance phase has been discussed or analyzed [2][3][6][7]. This paper especially focuses the effect of semicircular feet on inelastic collisions of heel-strike and theoretically investigates its mechanism through mathematical modeling of the collision. We first describe the detailed modeling of the heel-strike following inelastic collision law, and show that there exists a condition to make the energy dissipation be zero through analysis based on singular value decomposition. Throughout analyses, we show that semicircular feet with suitable foot radius function as a shock absorber for heel-strike.

F. Asano and Z.W. Luo are with Bio-Mimetic Control Research Center, RIKEN, Nagoya 463-0003, Japan asano@bmc.riken.jp

Z.W. Luo is with the Dept. of Computer and Systems Engineering, Faculty of Engineering, Kobe University, Kobe 657-8501, Japan luo@gold.kobe-u.ac.jp

II. Underactuated Virtual Passive Dynamic Walking

Before discussing the main subject, this section describes biped models with semicircular feet and underactuated virtual passive dynamic walking as an introduction of the effect of semicircular feet during the stance phase.

A. Compass-like biped model with semicircular feet

This paper treats a planar underactuated biped model with semicircular feet as shown in Fig. 1. The robot consists of two legs and three point masses, and has semicircular feet whose central points are on each leg. We assume that the stance-leg's foot is always in contact with the ground at exactly one point without slipping, that is, the rolling constraint condition is guaranteed. The dynamic equation is then derived as

$$\boldsymbol{M}(\boldsymbol{\theta})\ddot{\boldsymbol{\theta}} + \boldsymbol{C}(\boldsymbol{\theta},\dot{\boldsymbol{\theta}})\dot{\boldsymbol{\theta}} + \boldsymbol{g}(\boldsymbol{\theta}) = \boldsymbol{S}u_H = \begin{bmatrix} 1 \\ -1 \end{bmatrix} u_H \quad (1)$$

where $\boldsymbol{\theta} = \begin{bmatrix} \theta_1 & \theta_2 \end{bmatrix}^{\mathrm{T}}$ is the generalized coordinate vector and u_H is the hip-joint torque, respectively. The details of the terms were already explained in [3], so this paper omits them. Let E be the robot's total mechanical energy, its time-derivative then satisfies the relation $\dot{E} = \dot{\theta}_H u_H$ where $\theta_H := \theta_1 - \theta_2$ is the relative hip-joint angle.

B. Underactuated virtual passive dynamic walking

Asano *et al.* discovered that, in the case of virtual passive dynamic walking (VPDW) on level ground [5], the following relation holds between the mechanical energy and the X-position of CoM:

$$\dot{E} = Mg\tan\phi\dot{X}_g \quad (2)$$

where X_g [m] is the X-position at CoM, $M := m_H + 2m$ [kg] is the robot's total mass and ϕ [rad] is the virtual slope

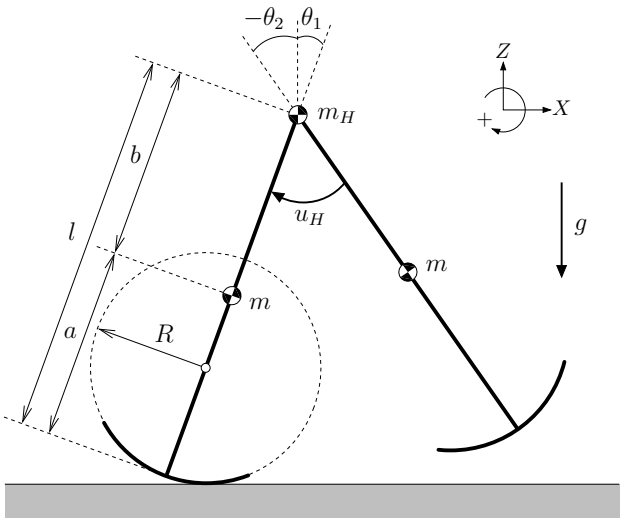

Fig. 1. Model of planar underactuated compass-like biped robot with semicircular feet

angle, respectively [5]. In the case with hip-joint actuation only, Eq. (2) yields the following form:

$$\dot{E} = \dot{\theta}_H u_H = Mg \tan\phi \dot{X}_g \tag{3}$$

and the hip-joint torque u_H is then determined uniquely as

$$u_H = \frac{Mg \tan\phi \dot{X}_g}{\dot{\theta}_H}. \tag{4}$$

Asano *et al.* showed that VPDW on level ground is impossible by hip-joint actuation only, whereas in the case with semicircular feet it becomes possible because the rolling effect dramatically increases the stable domain. We call the generated walking style by the control input of Eq. (4) "underactuated virtual passive dynamic walking (UVPDW)" in the following. The property of semicircular feet is that the rolling effect acts as the ankle-joint torque and drives the robot's CoM forward effectively.

By setting the origin as the contact point between the sole and the ground when $\theta_1 = 0$, the X-position of the robot's CoM is determined as

$$X_g = R(\theta_1 - \sin\theta_1) + \frac{(m_H l + ma + ml)\sin\theta_1 - mb\sin\theta_2}{M}, \tag{5}$$

and its time-derivative yields

$$\dot{X}_g = R\dot{\theta}_1(1-\cos\theta_1) + \frac{(m_H l + ma + ml)\dot{\theta}_1\cos\theta_1 - mb\dot{\theta}_2\cos\theta_2}{M}. \tag{6}$$

Note that the second term is the same as that of the flat feet model, and the first term is almost 0 if θ_1 is sufficiently small. This implies that the foot radius R does not directly affect the walking speed during the stance phase or its geometric effect is weak. The reason why the semicircular feet increases the walking speed does not lie in the rolling effect. We then investigate the effect on inelastic collisions by heel-strike deeply in the following sections.

C. Knees

By the rolling effect of semicircular feet, UVPDW is also realized by a kneed model. Fig. 2 shows the model of a planar kneed biped with semicircular feet, which consists of three links and four point masses. We assume that the knee-joint of stance leg is mechanically locked and does not rotates during the stance phase. The dynamic equation of the kneed biped is given by

$$\boldsymbol{M}(\boldsymbol{\theta})\ddot{\boldsymbol{\theta}} + \boldsymbol{C}(\boldsymbol{\theta},\dot{\boldsymbol{\theta}})\dot{\boldsymbol{\theta}} + \boldsymbol{g}(\boldsymbol{\theta}) = \boldsymbol{S}u_H = \begin{bmatrix} 1 \\ -1 \\ 0 \end{bmatrix} u_H, \tag{7}$$

where $\boldsymbol{\theta} = \begin{bmatrix} \theta_1 & \theta_2 & \theta_3 \end{bmatrix}^{\mathrm{T}}$. The gravity term of this kneed model is given by

$$\boldsymbol{g}(\boldsymbol{\theta}) = \begin{bmatrix} -(m_H l_1 + m_1 a_1 + m_2 l_1 + m_3 l_1)\sin\theta_1 \\ (m_2 b_2 + m_3 l_2)\sin\theta_2 \\ m_3 b_3 \sin\theta_3 \end{bmatrix} g + \begin{bmatrix} MRg\sin\theta_1 \\ 0 \\ 0 \end{bmatrix}, \tag{8}$$

and the first term of the right-hand side is the same as that of a flat feet model. Since other terms $\boldsymbol{M}$ and $\boldsymbol{C}\dot{\boldsymbol{\theta}}$ are equivalent to those of a flat feet model in the meaning of a linearized system, also in the kneed case, a semicircular feet model can be regarded as a flat feet model with ankle-joint torque given as $-MRg\sin\theta_1$. By using this effect, the kneed biped can also exhibit UVPDW on level ground by the hip-joint torque in Eq. (4). Fig. 3 shows the stick diagram of UVPDW where $\phi = 0.015$ [rad] and $R = 0.4$ [m], the physical parameter settings are omitted. Under the assumption that the knee-joint of swing leg is mechanically locked after the collision, at instant of heel-strike, the biped system can be treated as a two-linked model. We investigate the detailed mechanism of the two-linked collision model and the effect of semicircular feet on the mechanical energy dissipation in the following.

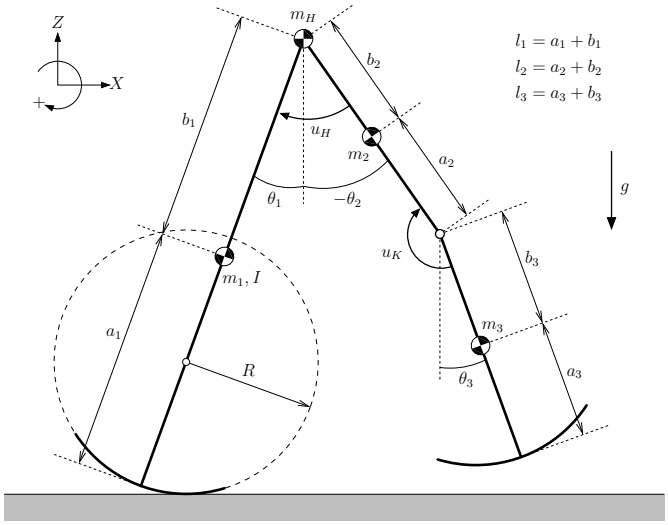

Fig. 2. Model of planar underactuated biped robot with semicircular feet and knee-joint

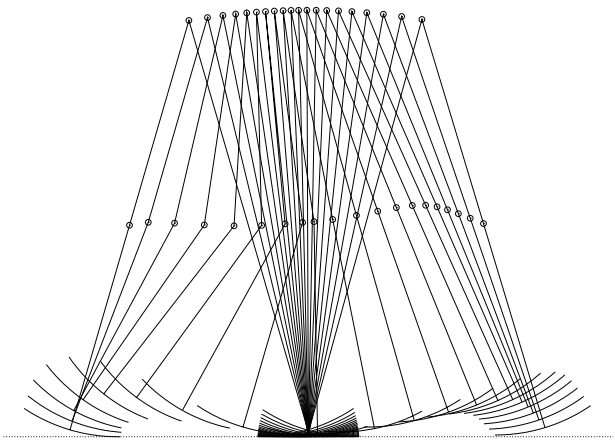

Fig. 3. Stick diagram for underactuated virtual passive dynamic walking with semicircular feet and knee-joint where $\phi = 0.015$ [rad] and $R = 0.4$ [m]

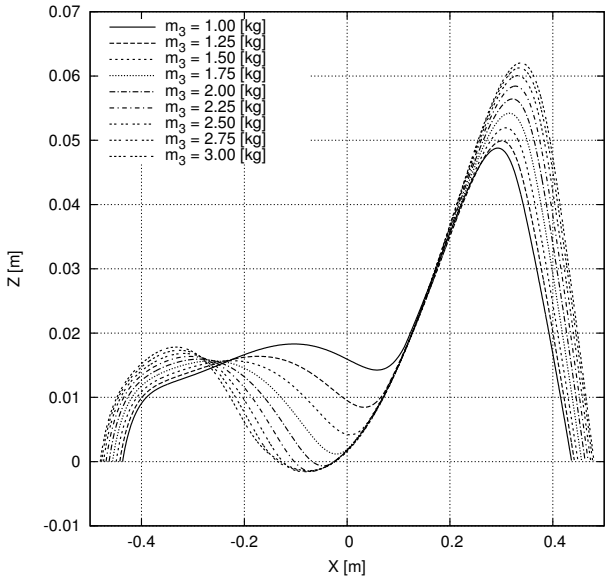

Fig. 4. Foot clearance for nine values of m_3 in underactuated virtual passive dynamic walking

Fig. 4 shows the lowest point of the sole to check the foot clearance with respect to the mass balance; various cases of m_3 is examined while maintaining $m_2 + m_3 = 5.0$ [kg]. In general, to guarantee the foot clearance during stance phase, the shin mass should be chosen sufficiently lighter than the thigh. We leave a detailed discussion about this for another opportunity, let's focus the lecture on the inelastic collision mechanism of heel-strike in the following sections.

III. Modeling Inelastic Collision

This section describes the inelastic collision model of heel-strike in detail.

A. Derivation of inelastic collision model and dissipated mechanical energy

The dynamic equation can be derived following Lagrange principle, whereas the transition equation for stance-leg exchange must be derived by extending the system's coordinate and introducing the corresponding generalized coordinate vector. Fig. 5 shows the geometric condition at instant of heel-strike; the two legs are symmetric. We call respectively the forward leg "Leg 1" and the rear one "Leg 2"; Leg 1 is the pre-stance leg and Leg 2 is the pre-swing leg. Define the extended coordinate vector of the Leg i, $\boldsymbol{q}_i \in R^3$, and that of the augmented system, $\boldsymbol{q} \in R^6$, respectively as

$$\boldsymbol{q}_i := \begin{bmatrix} x_i \\ z_i \\ \theta_i \end{bmatrix}, \quad \boldsymbol{q} := \begin{bmatrix} \boldsymbol{q}_1 \\ \boldsymbol{q}_2 \end{bmatrix}, \tag{9}$$

where x_i and z_i are X and Z-positions of the central point of semicircular feet. Under the assumption that the stance leg and the swing leg are switched instantaneously following inelastic collision law, the pre and the post angular positions of the original generalized coordinate satisfy the relations $\theta_1^- = \theta_2^+$ and $\theta_2^- = \theta_1^+$. Whereas in the extended coordinate $\boldsymbol{q}$, this change does not occur and $\boldsymbol{q}^+ = \boldsymbol{q}^- = \boldsymbol{q}$. In the following, the notation θ_i is of the extended coordinate. Considering this relation, the inelastic collision model can be formulated as

$$\bar{\boldsymbol{M}}(\boldsymbol{q})\dot{\boldsymbol{q}}^+ = \bar{\boldsymbol{M}}(\boldsymbol{q})\dot{\boldsymbol{q}}^- - \boldsymbol{J}_I(\boldsymbol{q})^{\mathrm{T}}\boldsymbol{\lambda}_I, \tag{10}$$

where $\boldsymbol{J}_I^{\mathrm{T}}\boldsymbol{\lambda}_I \in R^4$ stands for the impulsive force vector and $\boldsymbol{J}_I \in R^{4\times 6}$ is the Jacobian matrix which should satisfy the condition

$$\boldsymbol{J}_I(\boldsymbol{q})\dot{\boldsymbol{q}}^+ = \boldsymbol{0}_{4\times 1}. \tag{11}$$

$\bar{\boldsymbol{M}}(\boldsymbol{q}) \in R^{6\times 6}$ is the inertia matrix corresponding to the extended coordinate, $\boldsymbol{q}$, and detailed as

$$\begin{aligned}
\bar{\boldsymbol{M}}(\boldsymbol{q}) &= \begin{bmatrix} \boldsymbol{M}_1(\boldsymbol{q}_1) & \boldsymbol{0}_{3\times 3} \\ \boldsymbol{0}_{3\times 3} & \boldsymbol{M}_2(\boldsymbol{q}_2) \end{bmatrix}, \\
\boldsymbol{M}_i(\boldsymbol{q}_i) &= \begin{bmatrix} M_{i11} & 0 & M_{i13} \\ & M_{i22} & M_{i23} \\ \mathrm{Sym.} & & M_{i33} \end{bmatrix}, \\
M_{i11} &= M_{i22} = \frac{m_H}{2} + m, \\
M_{i13} &= \Big(\frac{m_H}{2}(l-R) + m(a-R)\Big)\cos\theta_i, \\
M_{i23} &= -\Big(\frac{m_H}{2}(l-R) + m(a-R)\Big)\sin\theta_i, \\
M_{i33} &= \frac{m_H}{2}(l-R)^2 + m(a-R)^2.
\end{aligned}$$

Here, note that matrix $\boldsymbol{M}_i$ differs in the case of kneed model because the stance leg has an inertia moment, I [kg·m^2], and M_{i33} therefore should be

$$M_{i33} = \frac{m_H}{2}(l-R)^2 + m(a-R)^2 + I.$$

The dissipated mechanical energy, ΔE_{hs} [J], is defined as

$$\Delta E_{\mathrm{hs}} = \frac{1}{2}\left(\dot{\boldsymbol{q}}^+\right)^{\mathrm{T}}\bar{\boldsymbol{M}}(\boldsymbol{q})\dot{\boldsymbol{q}}^+ - \frac{1}{2}\left(\dot{\boldsymbol{q}}^-\right)^{\mathrm{T}}\bar{\boldsymbol{M}}(\boldsymbol{q})\dot{\boldsymbol{q}}^- \leq 0. \tag{12}$$

$\boldsymbol{\lambda}_I \in R^4$ is Lagrange's undetermined multiplier vector within the context of impulsive force, and can be derived following Eqs. (10) and (11) as

$$\boldsymbol{\lambda}_I = \boldsymbol{X}_I^{-1}\boldsymbol{J}_I\dot{\boldsymbol{q}}^-, \quad \boldsymbol{X}_I := \boldsymbol{J}_I\bar{\boldsymbol{M}}^{-1}\boldsymbol{J}_I^{\mathrm{T}}. \tag{13}$$

By substituting this into Eq. (10), the post-impact velocity can be obtained as

$$\dot{\boldsymbol{q}}^+ = \left(\boldsymbol{I}_6 - \bar{\boldsymbol{M}}^{-1}\boldsymbol{J}_I^{\mathrm{T}}\boldsymbol{X}_I^{-1}\boldsymbol{J}_I\right)\dot{\boldsymbol{q}}^-. \tag{14}$$

In addition, the transformation from $\dot{\boldsymbol{q}}^+$ to $\dot{\boldsymbol{\theta}}^+$ is given by

$$\dot{\boldsymbol{\theta}}^+ = \begin{bmatrix} 0 & 0 & 0 & 0 & 0 & 1 \\ 0 & 0 & 1 & 0 & 0 & 0 \end{bmatrix}\dot{\boldsymbol{q}}^+. \tag{15}$$

Further substituting this into Eq. (12) and eliminating $\dot{\boldsymbol{q}}^+$, ΔE_{hs} can be simplified as

$$\Delta E_{\mathrm{hs}} = -\frac{1}{2}\left(\dot{\boldsymbol{q}}^-\right)^{\mathrm{T}}\boldsymbol{J}_I^{\mathrm{T}}\boldsymbol{X}_I^{-1}\boldsymbol{J}_I\dot{\boldsymbol{q}}^-. \tag{16}$$

Note that $\dot{\tilde{\boldsymbol{q}}}^-$ is given by transforming $\dot{\boldsymbol{q}}^-$ as

$$\begin{aligned}\dot{\tilde{\boldsymbol{q}}}^- &= \begin{bmatrix} R & 0 \\ 0 & 0 \\ 1 & 0 \\ R+(l-R)\cos\theta_1 & -(l-R)\cos\theta_2 \\ -(l-R)\sin\theta_1 & (l-R)\sin\theta_2 \\ 0 & 1 \end{bmatrix}\begin{bmatrix}\dot{\theta}_1^- \\ \dot{\theta}_2^-\end{bmatrix} \\ &=: \boldsymbol{H}(\boldsymbol{q})\dot{\boldsymbol{\theta}}^-. \end{aligned} \tag{17}$$

By using this relation, Eq. (16) is further simplified as follows:

$$\Delta E_{\mathrm{hs}} = -\frac{1}{2}\left(\dot{\boldsymbol{\theta}}^-\right)^{\mathrm{T}}\boldsymbol{H}^{\mathrm{T}}\boldsymbol{J}_I^{\mathrm{T}}\boldsymbol{X}_I^{-1}\boldsymbol{J}_I\boldsymbol{H}\dot{\boldsymbol{\theta}}^-. \tag{18}$$

Let α [rad] be the half inter-leg angle at the instant and is defined as

$$\alpha := \frac{\theta_1 - \theta_2}{2} > 0, \tag{19}$$

then the joint angles in Fig. 5 can be replaced by $\theta_1 = \alpha$ and $\theta_2 = -\alpha$, respectively. Note that the matrices $\boldsymbol{H}$, $\boldsymbol{J}_I$ and $\boldsymbol{X}_I$ are only functions of the angular positions. The following matrix

$$\boldsymbol{N} := \boldsymbol{H}^{\mathrm{T}}\boldsymbol{J}_I^{\mathrm{T}}\boldsymbol{X}_I^{-1}\boldsymbol{J}_I\boldsymbol{H} \in R^{2\times 2}, \tag{20}$$

is also only a function of α, and thus ΔE_{hs} can be expressed as

$$\Delta E_{\mathrm{hs}} = -\frac{1}{2}\left(\dot{\boldsymbol{\theta}}^-\right)^{\mathrm{T}}\boldsymbol{N}(\alpha)\dot{\boldsymbol{\theta}}^-. \tag{21}$$

B. Derivation of $\boldsymbol{J}_I$

This subsection describes the detailed derivation of $\boldsymbol{J}_I$. The configuration at instant of transition is shown in Fig. 2. The velocity constraint conditions between the two legs to connect them are derived from geometric conditions such that the Leg 1's hip is positioned the same as the Leg 2's, and they can be expressed as

$$x_1 + (l-R)\sin\theta_1 = x_2 + (l-R)\sin\theta_2, \tag{22}$$
$$z_1 + (l-R)\cos\theta_1 = z_2 + (l-R)\cos\theta_2. \tag{23}$$

Their time derivatives yield

$$\dot{x}_1^+ + (l-R)\dot{\theta}_1^+\cos\theta_1 = \dot{x}_2^+ + (l-R)\dot{\theta}_2^+\cos\theta_2, \tag{24}$$
$$\dot{z}_1^+ - (l-R)\dot{\theta}_1^+\sin\theta_1 = \dot{z}_2^+ - (l-R)\dot{\theta}_2^+\sin\theta_2. \tag{25}$$

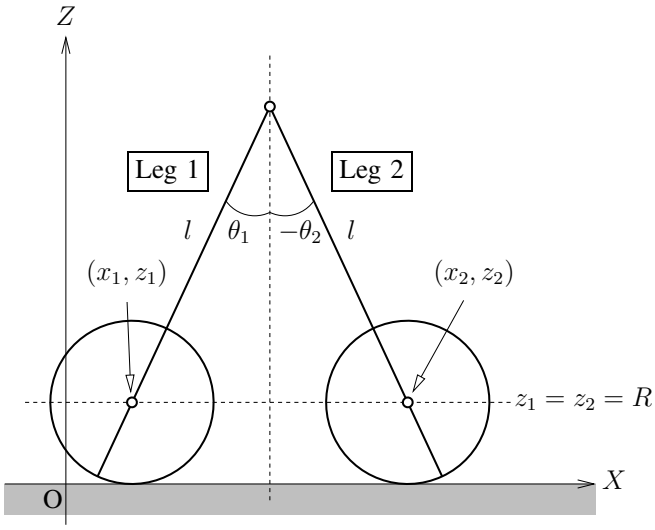

Fig. 5. Configuration at instant of heel-strike

Further, the rolling contact condition with the ground of the post-impact stance-foot is given by

$$\dot{x}_2^+ = R\dot{\theta}_2^+, \tag{26}$$
$$\dot{z}_2^+ = 0. \tag{27}$$

Summarizing the above four conditions, $\boldsymbol{J}_I$ yields

$$\boldsymbol{J}_I(\boldsymbol{q}) = \begin{bmatrix} 1 & 0 & (l-R)\cos\theta_1 & -1 & 0 & -(l-R)\cos\theta_2 \\ 0 & 1 & -(l-R)\sin\theta_1 & 0 & -1 & (l-R)\sin\theta_2 \\ 0 & 0 & 0 & 1 & 0 & -R \\ 0 & 0 & 0 & 0 & 1 & 0 \end{bmatrix}. \tag{28}$$

IV. Analysis based on singular value

Although the dissipated energy could be mathematically formulated, it is very difficult to analyze the detailed structure of ΔE_{hs} in Eq. (21). One candidate to evaluate the dissipative feature is the singular values of $\boldsymbol{N}$. The worst or the best cases of energy dissipation can be explained from the viewpoint of matrix norm induced by a vector 2-norm. The matrix $\boldsymbol{N}$ is always positive semi-definite and its singular value decomposition (SVD) has the form

$$\boldsymbol{N} = \boldsymbol{V}\boldsymbol{\Sigma}\boldsymbol{V}^{\mathrm{T}}, \quad \boldsymbol{\Sigma} = \begin{bmatrix}\sigma_1 & 0 \\ 0 & \sigma_2\end{bmatrix}. \tag{29}$$

Note that $\sigma_1 \geq \sigma_2 \geq 0$; the maximum and minimum singular values. $\boldsymbol{V} \in R^{2\times 2}$ is an Unitary matrix which should satisfy $\boldsymbol{V}^{\mathrm{T}}\boldsymbol{V} = \boldsymbol{V}\boldsymbol{V}^{\mathrm{T}} = \boldsymbol{I}_2$. The following relations hold between the induced 2-norm and the σ_1:

$$\|\boldsymbol{N}\|_2 = \left\|\boldsymbol{N}^{1/2}\right\|_2^2 := \sup_{\dot{\theta}^- \neq 0}\frac{\left\|\boldsymbol{N}^{1/2}\dot{\boldsymbol{\theta}}^-\right\|_2^2}{\left\|\dot{\boldsymbol{\theta}}^-\right\|_2^2} = \sigma_1(\boldsymbol{N}), \tag{30}$$

and the following equality also holds:

$$\frac{\left\|\boldsymbol{N}^{1/2}\dot{\boldsymbol{\theta}}^-\right\|_2^2}{\left\|\dot{\boldsymbol{\theta}}^-\right\|_2^2} = (\sigma_1 - \sigma_2)\cos^2\psi + \sigma_2, \tag{31}$$

TABLE I

PHYSICAL PARAMETERS OF THE ROBOT

m_H	10.0	kg
m	5.0	kg
$l\ (=a+b)$	1.0	m
a	0.5	m
b	0.5	m

where $\psi \in R$ is an arbitrary parameter. Eq. (31) then leads the following inequality:

$$\sigma_2(\boldsymbol{N}) \leq \frac{\left\| \boldsymbol{N}^{1/2}\dot{\boldsymbol{\theta}}^- \right\|_2^2}{\left\| \dot{\boldsymbol{\theta}}^- \right\|_2^2} \leq \sigma_1(\boldsymbol{N}). \tag{32}$$

Therefore, maximizing/minimizing the induced 2-norm of $\boldsymbol{N}$ means maximizing/minimizing the magnitude of the dissipated energy, $\Delta E_{\rm hs}$, for the given $\dot{\boldsymbol{\theta}}^-$.

Figs. 6 (a) and (b) show the maximum and minimum singular values of matrix $\boldsymbol{N}$ and their contours with respect to R and α where the physical parameters are chosen as Table I. As Fig. 6 (a) strongly indicates, the σ_1 monotonically decreases with the increase in R. This implies that semicircular feet decrease the energy dissipation in the case with large R, which can be understood from the viewpoint of that the walking system's dynamics closes to a wheel's one. It is another problem, however, whether or not a stable limit cycle is generated. There is a tendency that the gait becomes unstable and diverges as R closes to the leg length [3].

Note that, as seen in Fig. 6 (b), σ_2 is always 0 when $R = l$ or $\alpha = 0$. This means that there is a solution, $\dot{\boldsymbol{\theta}}^- \neq \boldsymbol{0}_{2\times 1}$, which achieves $\Delta E_{\rm hs} = 0$ in these cases. Let us derive its condition in the following.

Where $R = l$, matrix $\boldsymbol{N}$ has the form

$$\boldsymbol{N} = N_{R=l}\begin{bmatrix} 1 & -1 \\ -1 & 1 \end{bmatrix}, \quad \boldsymbol{\Sigma} = \begin{bmatrix} \sigma_1 & 0 \\ 0 & 0 \end{bmatrix},$$
$$\boldsymbol{V} = \begin{bmatrix} -1/\sqrt{2} & -1/\sqrt{2} \\ 1/\sqrt{2} & -1/\sqrt{2} \end{bmatrix}, \tag{33}$$

where

$$N_{R=l} = \frac{N_1}{N_2} > 0, \tag{34}$$
$$N_1 = 2mb^2l^2\left(m_H + m - m\cos(2\alpha)\right), \tag{35}$$
$$N_2 = 2m_Hl^2 + 3ml^2 + 2mb^2 - 4mbl\cos\alpha - ml^2\cos(2\alpha). \tag{36}$$

We can then solve the condition for $\Delta E_{\rm hs} = 0$. Substituting Eq. (33) into Eq. (21) gives

$$\begin{aligned}\Delta E_{\rm hs} &= -\frac{1}{2}\left\|\boldsymbol{\Sigma}^{1/2}\boldsymbol{V}^{\rm T}\dot{\boldsymbol{\theta}}^-\right\|^2 \\ &= -\frac{1}{2}\left\|\begin{bmatrix}\sqrt{\sigma_1} & 0 \\ 0 & 0\end{bmatrix}\begin{bmatrix}-1/\sqrt{2} & 1/\sqrt{2} \\ -1/\sqrt{2} & -1/\sqrt{2}\end{bmatrix}\begin{bmatrix}\dot{\theta}_1^- \\ \dot{\theta}_2^-\end{bmatrix}\right\|^2 \\ &= -\frac{1}{4}\sigma_1\left(\dot{\theta}_1^- - \dot{\theta}_2^-\right)^2. \end{aligned} \tag{37}$$

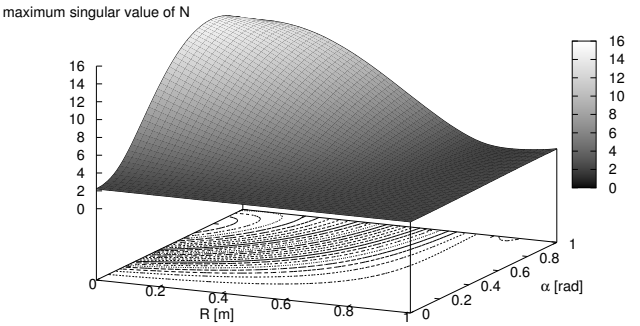

(a) maximum singular value σ_1 and its contours

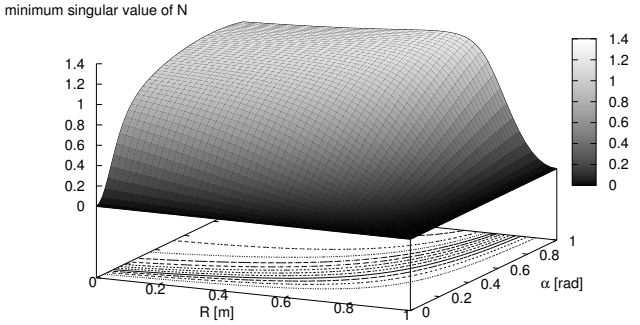

(b) minimum singular value σ_2 and its contours

Fig. 6. Singular values of matrix $\boldsymbol{N}$ and their contours with respect to R and α

Here, note that $\Delta E_{\rm hs}$ can also be derived following Eq. (21) as

$$\Delta E_{\rm hs} = -\frac{1}{2}N_{R=l}\left(\dot{\theta}_1^- - \dot{\theta}_2^-\right)^2, \tag{38}$$

and $2N_{R=l} = \sigma_1$ can be found. From Eqs. (37) and (38), we can conclude that the condition for $\Delta E_{\rm hs} = 0$ is $\dot{\theta}_1^- = \dot{\theta}_2^-$; the energy dissipation can be reduced to zero by controlling the pre-impact relative angular velocity of the hip-joint, 0 [rad/s], regardless of the physical parameter choice of the walking system.

McGeer studied this topic in his original work in 1990 [2], introducing a "synthetic wheel" with a mass-less leg. He pointed out that a synthetic wheel can *walk* on level ground without any power supply by choosing $R = l$ because support by the stance leg can roll seamlessly from one rim to the next. This is strongly supported by Eq. (35) because $\boldsymbol{N}$ becomes a zero matrix if $m = 0$. In addition, he remarked that the wheel should have a large point mass at the hip position, otherwise the swing-leg motion would disrupt the steady rolling. Considering real legged robots, this assumption is very hard to realize and we must conclude that the synthetic wheel is an extreme example and unrealistic.

Where $\alpha = 0$, matrix $\boldsymbol{N}$ can also be simplified and has

the form

$$\boldsymbol{N} = N_{\alpha=0} \begin{bmatrix} 1 & -1 \\ -1 & 1 \end{bmatrix}, \tag{39}$$

where

$$N_{\alpha=0} = \frac{m_H m b^2 l^2}{m_H l^2 + m a^2} \geq 0. \tag{40}$$

Since matrix $\boldsymbol{N}$ has the same form as $R = l$ in this case, the condition for $\Delta E_{\rm hs} = 0$ is $\dot{\theta}_1^- = \dot{\theta}_2^-$. Condition $\alpha = 0$ seems unrealistic and is not considered to be a suitable transition shape to generate a stable limit cycle.

Above analyses show that the optimal foot radius is $R = l$ in the meaning of minimizing the maximum singular value of $\boldsymbol{N}$. In the real legged robot design, however, we should choose a proper radius because the large R causes very long feet even if a high-speed walking would be realized.

V. Conclusions

This paper investigated the effect of semicircular feet on reducing mechanical energy dissipation by inelastic collisions of heel-strike. It has been clarified that, throughout analysis based on SVD, there is a tendency to decrease energy dissipation with the increase in the foot radius R and there is a condition to make the energy dissipation be zero when $R = l$; this result supports McGeer's original study of the synthetic wheel.

We can summarize the effect of semicircular feet on dynamic bipedal walking as follows.

- During the stance phase, semicircular feet provide the rolling effect which is equivalent to the ankle-joint torque.
- At instant of inelastic collisions of heel-strike, semicircular feet reduce the mechanical energy dissipation.

Multiple effects of both achieves an energy-efficient and high-speed dynamic biped locomotion. Optimal foot shape design of the convex curve is a subject left in future work. The mechanism to increase the stable domain of limit cycles is also an important problem to be theoretically clarified.

Traditionally, there has been a tendency to adopt flat feet in a biped humanoid robot design. The semicircular feet attached on the stance-leg, however, function as the ankle-joint torque during the stance phase virtually and as a shock absorber for heel-strike. The walking system's performance is as a result improved and the difficulty comes from the ZMP constraint also disappears. This fact suggests that it is necessary to reconsider biped robot mechanism with flat feet or ZMP-based approach.

VI. Acknowledgments

This work was partially supported by a Grant-in-Aid for Scientific Research, (B) No. 18360115, provided by the Japan Society for the Promotion of Science (JSPS).

References

[1] M. Vukobratović and J. Stepanenko, "On the stability of anthropomorphic systems," *Mathematical Biosciences*, vol.15, pp.1–37, 1972.

[2] T. McGeer, "Passive dynamic walking," *Int. J. of Robotics Research*, vol.9, no.2, pp.62–82, 1990.

[3] F. Asano and Z.W. Luo, "On energy-efficient and high-speed dynamic biped locomotion with semicircular feet," *Proc. of the IEEE/RSJ Int. Conf. on Intelligent Robots and Systems (IROS)*, pp.5901–5906, 2006.

[4] F. Asano and Z.W. Luo, "Dynamic analyses of underactuated virtual passive dynamic walking," *IEEE Int. Conf. on Robotics and Automation (ICRA)*, 2007, *to appear.*

[5] F. Asano, Z.W. Luo and M. Yamakita, "Biped gait generation and control based on a unified property of passive dynamic walking," *IEEE Trans. on Robotics*, vol.21, no.4, pp.754–762, 2005.

[6] R. Tedrake, T.W. Zhang, M. Fong and H.S. Seung, "Actuating a simple 3D passive dynamic walker," *Proc. of the IEEE Int. Conf. on Robotics and Automation (ICRA)*, pp.4656–4661, 2004.

[7] A. Chatterjee and M. Garcia, "Small slope implies low speed in passive dynamic walking," *Dynamics and Stability of Sytems*, vol.15, no.2, pp.139–157, 2000.